

Effect of reducing atmosphere on the magnetism of $\text{Zn}_{1-x}\text{Co}_x\text{O}$ ($0 \leq x \leq 0.10$) nanoparticles

M Naeem¹, S K Hasanain¹, M Kobayashi², Y Ishida²,
A Fujimori², Scott Buzby³ and S Ismat Shah³

¹ Department of Physics, Quaid-i-Azam University, Islamabad, Pakistan

² Department of Physics and Department of Complexity Science and Engineering, University of Tokyo, Kashiwa, Chiba 277-8561, Japan

³ Department of Physics and Astronomy, University of Delaware, Newark, Delaware 19716, USA

E-mail: skhasanain@qau.edu.pk

Received 4 January 2006, in final form 13 March 2006

Published 8 May 2006

Online at stacks.iop.org/Nano/17/2675

Abstract

We report the crystal structure and magnetic properties of $\text{Zn}_{1-x}\text{Co}_x\text{O}$ ($0 \leq x \leq 0.10$) nanoparticles synthesized by heating metal acetates in organic solvent. The nanoparticles were crystallized in the wurtzite ZnO structure after annealing in air and in a forming gas (Ar95% + H5%). The x-ray diffraction and x-ray photoemission spectroscopy (XPS) data for different Co content show clear evidence for the Co^{2+} ions in tetrahedral symmetry, indicating the substitution of Co^{2+} in the ZnO lattice. However, samples with $x = 0.08$ and higher cobalt content also indicate the presence of Co metal clusters. Only those samples annealed in the reducing atmosphere of the forming gas, that showed the presence of oxygen vacancies, exhibited ferromagnetism at room temperature. The air annealed samples remained non-magnetic down to 77 K. The essential ingredient in achieving room temperature ferromagnetism in these $\text{Zn}_{1-x}\text{Co}_x\text{O}$ nanoparticles was found to be the presence of additional carriers generated by the presence of the oxygen vacancies.

1. Introduction

The discovery of diluted magnetic semiconductors (DMSs), which are non-magnetic semiconductors doped with a small amount of some magnetic impurity, has raised tremendous interest in the development of these materials for future technological applications [1]. Due to its wide band gap (3.37 eV) and large excitation energy, transition-metal-doped ZnO has been investigated as a promising DMS for implementing spintronics device concepts [2]. One of the key questions is whether the resulting materials is indeed an alloy of $\text{Zn}_{1-x}\text{TM}_x\text{O}$ (TM = transition metal) or if on the other hand it remains as ZnO with clusters, precipitates, or with second phases that are responsible for the observed magnetic properties [3]. Since the appearance of the paper

by Dietl *et al* [4] predicting the existence of high temperature ferromagnetism (FM) in some magnetically doped wide band gap p-type semiconductors, much attention has been focused on these materials. In particular, ZnO and TiO_2 doped with different transition metals (Co, Mn, Fe, Ni, Cr, etc) have been the subject of intense research. Most of the theoretical models proposed so far assume TM ions as magnetic impurities and consider only p-type carriers, even though not all the compound semiconductors can be easily doped (without additional elements) with p-type dopants. While several groups have reported the synthesis of p-type ZnO by co-doping methods [5, 6], it is still difficult to dope ZnO with p-type dopants at high concentrations. Therefore the synthesis of ZnO with p-type TM doping is not convenient from a practical point of view. However, n-type conductivity is in general

more advantageous in potential technological applications [7]. Recent observations of a large anomalous Hall effect in n-type magnetic semiconductors such as Co-doped FeSi [8] and TiO₂ [9] suggest that ferromagnetic behaviour is also possible in n-type magnetic semiconductors. Thus it is important to search for suitable compositions of n-type ZnO-based DMSs, their preparation routes and the consequent electronic properties. The native defects in ZnO such as oxygen vacancies (V_o), zinc vacancies (V_{Zn}) and oxygen (O_i) and zinc interstitials (Zn_i) are understood to be fundamental sources of electron doping [10]. For example, the presence of V_o generates free carriers (electrons) that may help in mediating the exchange interaction effects between magnetic impurities. Furthermore, since the spintronic applications envisaged for DMS materials will require miniaturization [11], it is very important to understand the control and variation of the magnetic properties in these systems at the nanoscale. In this study we have investigated Co-doped ZnO-based DMS nanoparticles for room temperature ferromagnetism. The observation of ferromagnetism at room temperature is examined in the context of the substitution of Co in the lattice and the effects of the annealing environment. We present evidence from x-ray diffraction and x-ray photoemission spectroscopy (XPS) for the presence of Co in the substituted state up to a certain maximum concentration and for the crucial dependence of the observed ferromagnetism on the presence of V_o generated by annealing in a reducing atmosphere.

2. Experimental details

Nanoparticles of $Zn_{1-x}Co_xO$ ($x = 0-0.10$) were synthesized by heating metal acetates in organic solvent following the reported procedure [12]. Zinc acetate dihydrate $Zn(CH_3COO)_2 \cdot 2H_2O$ and cobalt acetate tetrahydrate $Co(CH_3COO)_2 \cdot 2H_2O$ were dispersed in a specific volume of ethyleneglycol (200 ml), and the overall metal concentration was controlled at 0.1 M. The suspension was stirred for about 30 min and heated at 200 °C for 3 h. A blue-green suspension of the oxide was observed for temperatures (T) above 180 °C. After the precipitation of the oxide, the mixture was cooled down to room temperature. The solid phase was recovered by centrifugation, washed repeatedly with ethanol and finally dried in air at 70 °C. For each concentration of Co, samples were annealed in air and the forming gas (Ar95% + H5%). The sample, contained in a quartz boat, was placed inside the tubular furnace and forming gas of purity 99.9% was passed over the samples at 600 °C. The structural characterizations were performed by powder x-ray diffraction (XRD) using Cu $K\alpha$ radiation $\lambda = 1.5405 \text{ \AA}$. The samples were also characterized by transmission electron microscopy (TEM) and x-ray photoemission spectroscopy (XPS). XPS measurements were performed using a Gammatdata Scienta SES-100 hemispherical analyser and an Al $K\alpha$ ($h\nu = 1486.6 \text{ eV}$) x-ray source in a vacuum below 1.0×10^{-9} Torr at room temperature. The escape depth of the Co 2p photoelectron was about 10 nm, with a beam size of about 1 mm. Pelletized samples were used for the XPS measurement and clean surfaces were obtained by scraping *in situ* with a diamond file. A vibrating sample magnetometer (VSM) was used to investigate the magnetic properties.

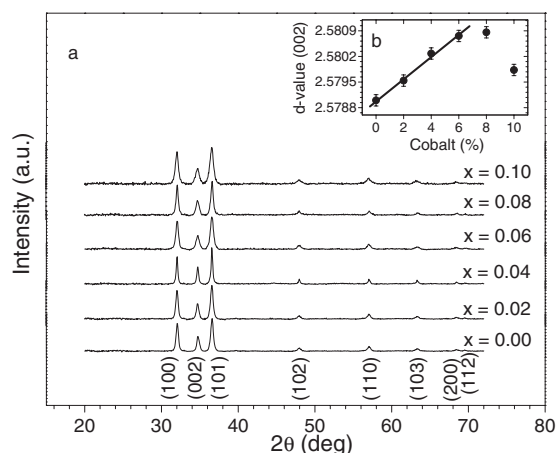


Figure 1. (a) X-ray diffraction patterns of $Zn_{1-x}Co_xO$ ($x = 0.00, 0.02, 0.04, 0.06, 0.08, 0.10$) nanoparticles. (b) Variation of $d(002)$ values versus Co concentration.

3. Results and discussion

XRD data of as prepared samples (data not shown) did not show any Bragg peaks, indicating that all as-prepared samples were amorphous. However, when the samples were annealed at 600 °C in air or in the forming gas, dominant features of a single phase with a hexagonal wurtzite structure were observed, as shown in figure 1(a). No unidentified peaks were seen in the data. The average particles size for all compositions is about 22 nm, as determined from x-ray line broadening using the Scherrer formula $D_{hkl} = K\lambda/\beta_{hkl} \cos \theta$, where D_{hkl} is the particle diameter in angstroms, K is the Scherrer coefficient, equal to 0.89, β is the full width at half maximum, and λ is the wavelength of the x-rays. From these measurements no traces of cobalt metal or cobalt oxides were detectable in any of our doped samples.

The typical detection limit of our system for an impurity phase is estimated as 2–4% of the total volume. The position of the XRD peak corresponding to the (002) plane is seen to be shifted towards lower 2θ values with increasing Co content up to $x = 0.06$. The $d(002)$ values from this peak are plotted as a function of Co content in the inset of figure 1. The lattice $d(002)$ spacing is observed to increase linearly with increasing Co content up to $x = 0.06$, consistent with other reported results on this systems [13, 14]. A linear increase of the lattice spacing thus indicates, in accordance with Vegard's law, that at least up to $x = 0.06$, Co ions are substituted in ZnO without changing the wurtzite structure. On further doping of Co (at $x \geq 0.08$) there is a clear decrease of the lattice constant with increasing Co content, suggestive of the presence of Co metal clusters. (These may be in addition to the Co ions present in a substitutional role in the ZnO lattice.) The bright field transmission electron microscopy (TEM) image, figure 2, shows that the samples consist generally of round faceted particles with typical particle size ranging between 20 and 50 nm, but larger size particles are also visible.

XPS studies were conducted to confirm the possible oxidation states of Co ion in the ferromagnetic $Zn_{1-x}Co_xO$ wurtzite structure of the nanoparticles. Figure 3 shows high resolution Co 2p XPS spectra of $Zn_{1-x}Co_xO$, for $x = 0.06$,

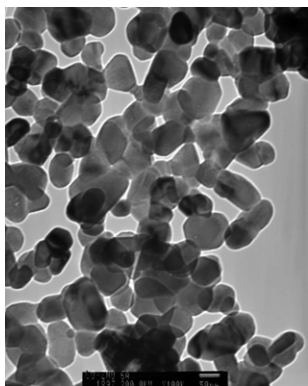


Figure 2. TEM image of $\text{Zn}_{0.94}\text{Co}_{0.06}\text{O}$ nanoparticles.

0.08, 0.10. Due to weak signal intensities, it was difficult to resolve the peaks for low Co composition samples. All of these samples show four peaks: the $2p_{3/2}$ and $2p_{1/2}$ doublet and the shake up resonance transitions (satellite) of these two peaks at higher binding energies. The Co $2p_{3/2}$ and $2p_{1/2}$ binding energies are obtained as 781.5 and 797 eV, respectively. These binding energies are very close to those reported for Co^{2+} ions in CoO [15]. In our case the difference of binding energies between the $2p_{3/2}$ and $2p_{1/2}$ levels is determined to be 15.5 ± 0.1 eV, which corresponds well with the value for Co^{2+} homogeneously surrounded by oxygen tetrahedra [16, 17]. If Co had existed largely in the form of metal clusters in these samples, the energy difference of these peaks would have been 15.05 eV [17]. Therefore, while the presence of Co clusters cannot be ruled out entirely, it appears that at least up to $x = 0.06$ the number of Co atoms involved in such clustering is at best too small to be detected by XPS. Given our beam size (1 mm) and the escape depth (10 nm), it is estimated that the system is capable of a detection limit of 500 ppm. However, for samples with $x \geq 0.08$, a shoulder starts to appear on the lower energy side of the Co $2p_{3/2}$ peak. This shoulder appears at a binding energy ~ 778 eV below the Co $2p_{3/2}$ peak in figure 3. Generally, core-level binding energy increases with increasing positive valence of the ion [18]. It is considered that the Co $2p$ peak appearing on the lower binding energy side indicates the presence of Co metal clusters. Our data for $x \geq 0.08$ therefore suggest that along with the Co^{2+} ions in the Zn substituted positions (CoO), there is also some Co in the form of metallic clusters.

Due to the pronounced difference between the magnetic response of the samples annealed in air and in the forming gas, respectively (discussed later), we investigated the presence of oxygen vacancies in the XPS spectra. In figure 4 we present the O 1s XPS spectra of $\text{Zn}_{0.94}\text{Co}_{0.06}\text{O}$. This is the composition with the largest Co content exhibiting no signatures of clustering, both in XRD and XPS. The O 1s XPS spectra of both air annealed (figure 4(a)) and forming gas annealed samples (figure 4(b)) show a slightly asymmetric peak very close to 530 eV. This profile can be fitted by two symmetrical peaks, which are normally assigned as the low binding energy component (LBEC) and the high binding energy component (HBEC), and it has been shown [19] that the HBEC peak develops with increasing loss of oxygen such as by heating in vacuum or by Ar^+ bombardment. The development

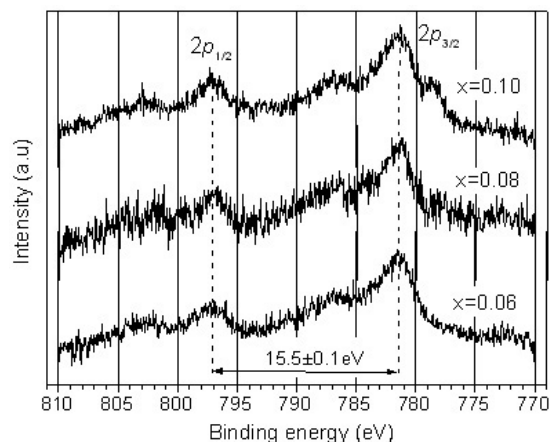


Figure 3. XPS spectra of Co $2p$ core levels as a function of Co concentration ($x = 0.06, 0.08, 0.10$) recorded at room temperature.

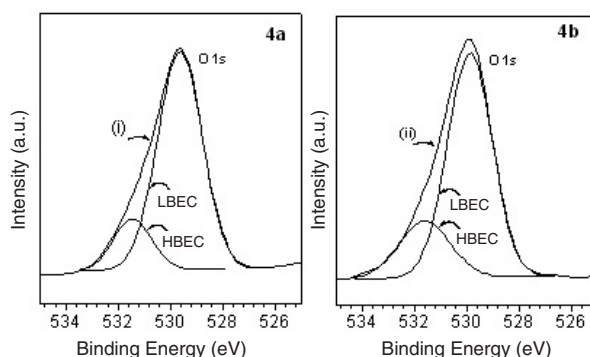


Figure 4. XPS spectra of O 1s core level recorded from the samples (a) annealed in air and (b) annealed in forming gas. Fits to the data of curves (i) and (ii) yield the two peaks LBEC and HBEC for each case (see text for details).

of the HBEC peak obviously leads to the asymmetry of the main peak (LBEC). Our O 1s x-ray photoemission spectra yield one clear observation, namely the asymmetry of the LBEC is found to be more pronounced in the samples annealed in forming gas as compared to the samples annealed in air. Furthermore, the relative area under the curve (area of HBEC peak/area of LBEC) is determined to be 0.281 ± 0.002 , while for the air annealed samples it is equal to 0.191 ± 0.001 . The relatively large contribution of the HBEC peak for the case of annealing in forming gas strongly suggests the presence of more oxygen deficiencies in this case. This is most probably due to the desorption of loosely bound oxygen during annealing in the reducing atmosphere of the forming gas. These oxygen vacancies are expected to generate free carriers (electrons) that can help in mediating the exchange interaction effects between the magnetic impurities.

We now turn to the magnetic properties of $\text{Zn}_{1-x}\text{Co}_x\text{O}$ nanoparticles. The samples annealed in air exhibited no ferromagnetic component down to 77 K, the lowest temperature investigated. Interestingly, however, after annealing in the forming gas at 600 °C all samples acquired room temperature ferromagnetism without any observable change in the crystal structure, as revealed by x-ray diffraction,

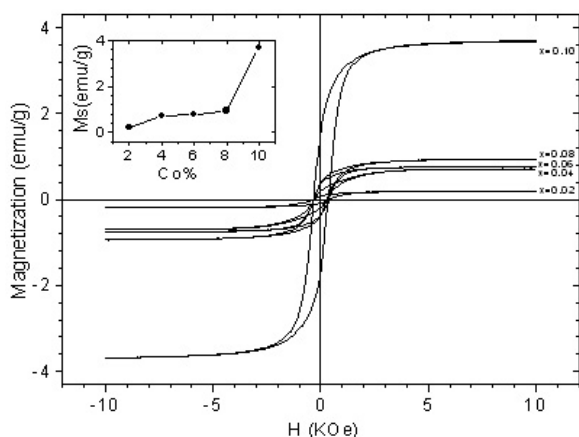


Figure 5. The $M-H$ curve of Co-doped ZnO nanoparticles measured at 300 K for different Co concentrations. Inset: Co content (x) dependence of M_s (emu g^{-1}).

or in the electronic structure observed by the XPS. This is unlike the case for Co-doped TiO_2 , where a reducing atmosphere helps in stabilizing the anatase phase that leads to ferromagnetism. The field-dependent magnetization ($M-H$) curves, at room temperature, of all five compositions are shown in figure 5. All samples exhibit room temperature FM with the moment (emu g^{-1}) monotonically increasing with increasing concentration of cobalt. The maximum saturation magnetization (M_s) was found to be 3.9 emu g^{-1} (10% Co doped) among all compositions, while the maximum moment per Co atoms was $\mu \sim 0.25 \mu_B/\text{Co}$ (4% Co doped) at room temperature. The values range between 0.141 ($x = 0.02$) and $0.533 \mu_B/\text{Co}$ ($x = 0.10$). These values are comparable with those typically reported in the literature [20]. It is noticeable however that the value of M_s in our case was quite small (maximum $0.533 \mu_B/\text{Co}$) in comparison with the value $\mu = 3\mu_B/\text{Co}$ expected from the moment of ionic Co^{2+} in a tetrahedral crystal field. Some authors have attributed the much less than saturation values for the moment as originating in the presence of additional antiferromagnetic-type couplings between some of the neighbouring ions [21] that may lead to a canting of the spins. The reduced value could also be reflective of the fact that even at 10% doping level, where substitutional and metallic Co still coexist, the ferromagnetic moment is not stabilized for all the Co ions and the measured moment is obviously an average over all such ions.

A large jump in the magnetic moment is observed at $x = 0.10$ shown in inset of figure 5. The large moment at $x = 0.10$ may be related, as evidenced by the XPS spectra, to the formation of Co clusters with strong ferromagnetic alignment. In the $x = 0.08$ composition (which appears to be a borderline composition on the basis of magnetization and structural studies) we could also have the possibility of coexistence of divalent Co ions and Co metal clusters as observed in the Co 2p XPS spectra. However, in the composition range $x \leq 0.06$, where Co was seen to be substituted in the ZnO matrix, the observed ferromagnetic component appears to be arising from Co ions randomly substituted for Zn in the ZnO matrix. The FM correlations in this composition range, where Co ions may be regarded as being generally randomly

distributed, appear to be connected with the excess electrons arising from the oxygen vacancies [10]. Theoretically, it has been observed that the carrier-mediated ferromagnetism in n-type oxide semiconductors is strongly related to the presence of oxygen vacancies [22]. Whether this indirect exchange interaction is of the RKKY type or due to some other mechanism, e.g. virtual magnetic levels [20] close to the band edge, is not understood at the moment.

The moment per Co atom, as mentioned earlier, varies between 0.14 and $0.254 \mu_B/\text{Co}$ for the range where Co ions appear to go in substitutionally, with the 8% doping samples having a moment of $0.16 \mu_B/\text{Co}$. The current study is not able to give an explanation of these variations but aims to highlight the abrupt change at 10% doping levels for which both the XPS and XRD studies also give clear indications of the presence of metal clustering. A similar abrupt jump in the moment has been reported [23] and has also been attributed to the formation of cobalt metal clusters. It is noted however that the value of the Co moment is not expected in general to be a monotonic function of Co concentration since it is the presence of the additional carriers that is responsible for the stabilization of the ferromagnetic state [24]. The ultimate free carrier density is expected to be a function both of the reducing atmosphere that generates carriers *as well as* the extent of the formation of the Co^+ ions that are understood as forming the shallow dopant states which in the view of some authors [25] leads to a spin-dependent hopping between the ions of the double exchange type. Other authors [26] have identified the hybridization of the Co^{2+} and the Co^{1+} as the source of the stabilization of the FM moment.

The coercive field (H_c) of 6% Co-doped samples was found to be 320 Oe at room temperature, as shown in figure 4. In thin film samples of similar compositions [16], the coercivity values are much smaller, being typically a few tens of oersteds. The relatively large values we observe are very definitely due to the single domain nature of these nanoparticles and the associated magnetization rotation magnetic mechanism [27]. In nanoparticles, the formation of domain walls is energetically unfavourable below a certain size, depending on the materials, and the particle stays in a single domain configuration. In a single domain particle, magnetization reversal can occur only by magnetization rotation (as opposed to domain wall motion), requiring large reversing fields.

Figure 6 shows zero field cooled (ZFC) and field cooled (FC) magnetization data as a function of temperature for the $x = 0.06$ sample in different fields. In the field cooled case the field was applied at room temperature and the data were taken on the way down, while in the ZFC case the sample was cooled down to the lowest temperature of the study in zero applied field and then warmed up in an applied field. It is understood that for ZFC magnetic nanoparticles [28] if the applied field is not large enough most of the particles have their moments blocked along their respective anisotropy axes, yielding low susceptibility and moments. With increasing temperatures the particles get increasingly unblocked from their anisotropy directions, yielding an *increase* in the moment and susceptibility. At a characteristic temperature T_B the effects of field and temperature become dominant over the anisotropy effects and the moments begin to depict a

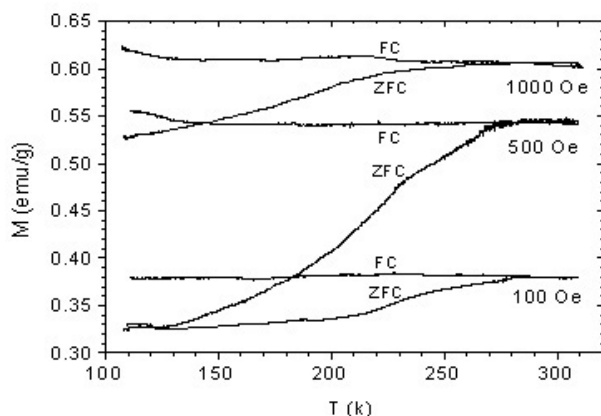


Figure 6. M - T curves of $\text{Zn}_{0.94}\text{Co}_{0.06}\text{O}$ nanoparticles at three different magnetic fields.

paramagnetic-like *decrease* and enter the superparamagnetic state. For the FC case when the field is applied at high enough temperatures where the moments are unblocked the magnetic response does not decrease with decreasing temperature. The coincidence of the maximum of the ZFC and the point of merger of the FC and ZFC curves is understood as reflecting the narrowness of the particle size distribution. The FC and ZFC curves (figure 6) are seen to diverge substantially at low temperatures, with the FC data being quite temperature independent for the most part, while the zero field data show a broad maximum. This maximum progressively shifts to a lower temperature with increasing magnetic field (H). This field dependence of the ZFC maximum is consistent with that expected for magnetic nanoparticles [28] where larger fields prevent blocking and shift the blocking to lower temperatures. The presence of a large hysteresis even at room temperature indicates that the blocking temperature (and hence the critical temperature) for most of the particles is substantially higher than 300 K. Differences between ZFC and FC could in principle also arise due to spin-glass-type ordering within or between the particles at low temperatures [29]. However, the very broad ZFC peak even at the lowest applied field (100 Oe) is typical of spin blocking in nanoparticles with a size distribution and unlike that for a typical spin glass.

Two other features are noticeable in the $M(T)$ data. First, there is the very large difference between the ZFC values between $H = 100$ and 500 Oe at room temperature and their coincidence at low temperatures. We understand this large difference at room temperature as occurring due to the value of the applied field exceeding the threshold of 320 Oe (H_c) in this range. For a 100 Oe applied field ($H < H_c$) the field is not sufficient to align most of the particles while the 500 Oe field is quite sufficient. However, at low temperatures (say 110 K) the coercive field is about 650 Oe and both the applied fields (100 and 500 Oe) are smaller than the coercivity and the consequent moments are very small and almost the same. Second, we observe a slight but significant and reproducible upturn in the FC moment at the lowest temperatures, $T < 150$ K, for the higher fields, 500 and 1000 Oe. This appears to be similar to the case of magnetic nanoparticles [30] with a surface layer that undergoes an ordering at low enough temperatures, stabilized by the high magnetic fields. A similar explanation may be valid

here as well. Further experiments are underway to identify the origins of this low temperature behaviour.

4. Conclusion

In conclusion, the structure and magnetic properties of $\text{Zn}_{1-x}\text{Co}_x\text{O}$ ($0 \leq x \leq 0.10$) nanoparticles synthesized by heating metal acetate in organic solvent were studied. No secondary phase was observed in the XRD patterns in the whole range of compositions ($0 \leq x \leq 0.10$). The $d(002)$ value evolution and XPS spectra revealed that the Co ions in $\text{Zn}_{1-x}\text{Co}_x\text{O}$ for $x \leq 0.06$ are in the divalent Co^{2+} states with a tetrahedral symmetry. Hence both the structure and the magnetic properties provide strong evidence that the Co ions are substituted in ZnO matrix up to $x \leq 0.06$. The stark contrast in the magnetic response of the particles annealed in the forming gas to those annealed in air clearly shows that the generation of additional carriers by the oxygen vacancies plays a crucial role, most likely in mediating the exchange interaction between the Co ions. The magnetic behaviour of the nanoparticle assembly is consistent with that for a collection of magnetic nanoparticles undergoing blocking along the anisotropy axes, and there is evidence of a low temperature ordering of moments possibly in the outer shell of the particles.

Acknowledgment

The work at Quaid-i-Azam University was supported by a research grant No. 20-80/Acad(R)/03 from the Higher Education Commission of Pakistan.

References

- [1] Pearton S J *et al* 2003 *J. Appl. Phys.* **93** 1–13 and reference therein
- [2] Roy V A, Djuricic L A B, Liu H, Zhang X X, Leung Y H, Xie M H, Gao J, Lui H F and Surya C 2004 *Appl. Phys. Lett.* **84** 756–67
- [3] Ogale S B *et al* 2003 *Phys. Rev. Lett.* **91** 0772051
- [4] Dietl T, Ohno H, Matsukura M, Cibert J and Ferrand D 2000 *Science* **287** 1019–22
- [5] Yamamoto T and Yoshida H K 1999 *Japan. J. Appl. Phys.* **38** L166–9
- [6] Joseph M, Tabata H and Kawai T 1999 *Japan. J. Appl. Phys.* **38** L1205–7
- [7] Pearton S 2004 *Nat. Mater.* **3** 203–4
- [8] Manyala N *et al* 2004 *Nat. Mater.* **3** 255–62
- [9] Toyosaki H *et al* 2004 *Nat. Mater.* **3** 221–4
- [10] Zhange S B, Wei S-H and Zunger A 2001 *Phys. Rev. B* **63** 0752051
- [11] Ronning C, Gao P X, Ding Y, Wang Z L and Schwen D 2004 *Appl. Phys. Lett.* **84** 783–5
- [12] Poul L, Ammar S, Jouini N, Fievet F and Villain F 2001 *Solid State Sci.* **3** 31–42
- [13] Risbud A S, Spaldin N A, Chen Z Q, Stemmer S and Seshadri R 2003 *Phys. Rev. B* **68** 2052021
- [14] Cong C J, Liao L, Li J C, Fan L X and Zhang K L 2005 *Nanotechnology* **16** 981–4
- [15] Shen Z X *et al* 1990 *Phys. Rev. B* **42** 1817–28
- [16] Lee H J, Jeong S Y, Cho C R and Park C H 2002 *Appl. Phys. Lett.* **81** 4020–2
- [17] Wagner C D *et al* 1979 *Handbook of X-ray Photoelectron Spectroscopy* (Minnesota, USA: Perkin-Elmer) p 78

- [18] Hufner S 2003 *Photoelectron Spectroscopy, Principles and Applications* (Berlin: Springer)
- [19] Tyuliev G and Angelov S 1988 *Appl. Surf. Sci.* **32** 381–91
- [20] Yang S G, Pakhomov A B, Hung S T and Wong C Y 2002 *IEEE Trans. Magn.* **38** 2877–9
- [21] Ohno H J 1999 *Magn. Mater.* **200** 110–29
- [22] Park M S, Kwon S K and Min B I 2002 *Phys. Rev. B* **65** 161201
- [23] Deka S and Joy P A 2005 *Solid State Commun.* **134** 665–9
- [24] Spaldin N A 2004 *Phys. Rev. B* **69** 125201
- [25] Schwartz D A and Gamelin D R 2004 *Adv. Mater.* **16** 2115–9
- [26] Kittilstved K R, Liu W K and Gamelin D R 2005 *Preprint cond-mat/0510644*
- [27] Stoner S C and Wohlfarth E P 1948 *Phil. Trans. R. Soc. A* **240** 599
- [28] Shinde S R *et al* 2004 *Phys. Rev. Lett.* **92** 166601
- [29] Shand P M, Christianson A D, Pekarek T M, Martinson L M, Schweitzer J W, Miotkowski I and Crooker B C 1998 *Phys. Rev. B* **58** 12876–82
- [30] Baker C, Hasanain S K and Shah S I 2004 *J. Appl. Phys.* **96** 6657–62